

Perspective: Emergent topologies in oxide superlattices

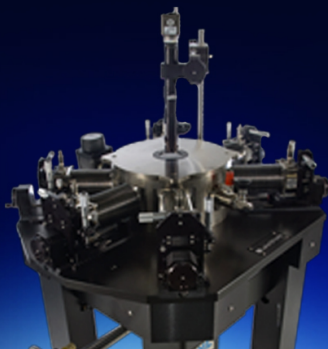
Sujit Das, Anirban Ghosh, Margaret R. McCarter, Shang-Lin Hsu, Yun-Long Tang, Anoop R. Damodaran, R. Ramesh, and Lane W. Martin

Citation: [APL Materials](#) **6**, 100901 (2018); doi: 10.1063/1.5046100

View online: <https://doi.org/10.1063/1.5046100>

View Table of Contents: <http://aip.scitation.org/toc/apm/6/10>

Published by the [American Institute of Physics](#)



Cryogenic probe stations

for accurate, repeatable
material measurements

Perspective: Emergent topologies in oxide superlattices

Sujit Das,¹ Anirban Ghosh,¹ Margaret R. McCarter,² Shang-Lin Hsu,^{1,2,3}
Yun-Long Tang,⁴ Anoop R. Damodaran,¹ R. Ramesh,^{1,2,4}
and Lane W. Martin^{1,4,a}

¹Department of Materials Science and Engineering, University of California, Berkeley, California 94720, USA

²Department of Physics, University of California, Berkeley, California 94720, USA

³National Center for Electron Microscopy, Molecular Foundry, Lawrence Berkeley National Laboratory, Berkeley, California 94720, USA

⁴Materials Sciences Division, Lawrence Berkeley National Laboratory, Berkeley, California 94720, USA

(Received 25 June 2018; accepted 8 August 2018; published online 24 October 2018)

The ability to synthesize high-quality, complex-oxide heterostructures has created a veritable playground in which to explore emergent phenomena and exotic phases which arise from the interplay of spin, charge, orbital, and lattice degrees of freedom. Of particular interest is the creation of artificial heterostructures and superlattices built from two or more materials. Through such approaches, it is possible to observe new phases and phenomena that are not present in the parent materials alone. This is especially true in ferroelectric materials where the appropriate choice of superlattice constituents can lead to structures with complex phase diagrams and rich physics. In this article, we review and explore future directions in such ferroic superlattices wherein recent studies have revealed complex emergent polarization topologies, novel states of matter, and intriguing properties that arise from our ability to manipulate materials with epitaxial strain, interfacial coupling and interactions, size effects, and more. We focus our attention on recent work in $(\text{PbTiO}_3)_n/(\text{SrTiO}_3)_n$ superlattices wherein exotic polar-vortex structures have been observed. We review the history of these observations and highlights of recent studies and conclude with an overview and prospectus of how the field may evolve in the coming years. © 2018 Author(s). All article content, except where otherwise noted, is licensed under a Creative Commons Attribution (CC BY) license (<http://creativecommons.org/licenses/by/4.0/>). <https://doi.org/10.1063/1.5046100>

INTRODUCTION—INTERFACES ABOUND

Complex-oxide materials and their heterostructures have garnered enormous interest in the last decade because of the potential for and realization of exotic phenomena, including emergent interfacial conduction, magnetic order, superconductivity, new ferroelectric order, etc. Made possible by advances in material synthesis, such heterostructures and heterointerfaces provide for a rich array of interesting physics and properties that hold promise for future technologies.^{1–3} One of the most prominent examples in this regard is the conductivity that emerges at the interfaces between two large bandgap insulating oxides, LaAlO_3 and SrTiO_3 .^{4,5} Regardless of the system, it has been shown that the interfaces themselves and the subsequent coupling between adjacent layers are of utmost importance and ultimately govern the properties of the heterostructures. Such heterointerfaces in complex-oxide systems have been shown to exhibit novel functionalities, which can be completely different from those of the respective bulk materials, and their behavior can be tuned by varying the composition, temperature, pressure, strain, and much more.^{6–10} The same holds true in ferroic (i.e., magnetic, ferroelectric, multiferroic) systems. For instance, the emergence of ferromagnetism between two non-magnetic materials has been explained by the ability to atomically control

^aE-mail: lwmartin@berkeley.edu

materials in such a way that they drive heterointerfacial superexchange interactions that change the local properties.¹¹ Leveraging this ability to control materials, researchers have gone on to observe antiferromagnetic coupling at ferromagnetic/ferromagnetic interfaces¹² and exchange-bias coupling in paramagnetic/ferromagnetic¹³ and ferromagnetic/antiferromagnetic interfaces.¹⁴ Such magnetic interfaces nicely illustrate the richness of interfacial coupling phenomena, many of which are important from a technological perspective (e.g., in magnetic sensors, read-write heads, ultrahigh density memory devices, and spintronic applications).¹⁵ At the same time, studies of magnetoelectric coupling effects in multiferroics and heterostructures of magnetic and ferroelectric/piezoelectric materials provide novel approaches to realize emergent functions like electric-field control of magnetism.^{16–18} For example, carrier-mediated magnetoelectric effects have been observed at metal/ferroelectric heterointerfaces (e.g., $\text{La}_{1-x}\text{Sr}_x\text{MnO}_3/\text{PbZr}_{1-x}\text{Ti}_x\text{O}_3$), where the magnetic state can be modulated by the accumulation of charge carriers in the ferroelectric layer due to an applied field.¹⁸ Such systems are promising for information technology devices,¹⁹ electrically controlled magnetic data storage,²⁰ and magnetically operated electric devices.²¹ What are the open questions in this field? By far, the most important of them would be to understand the fundamental limits of the coupling and charge transfer at the interfaces. This would then be a pathway to enhance the magnitude of the coupling such that measurable directional exchange coupling is possible.

The final type of interfacial effects in ferroic systems that we will touch upon is the emergent new properties in heterostructures based on ferroelectric materials. The local atomic and mesoscopic domain structures that arise in such ferroelectric heterostructures strongly affect the dielectric, piezoelectric, and optical properties of ferroelectric thin films,²² and such structures can be controlled by manipulation of the elastic and electrostatic energies of the system. For example, the polarization and, in turn, the electrical properties of tricolor $\text{PbTiO}_3/\text{SrTiO}_3/\text{PbZr}_{0.2}\text{Ti}_{0.8}\text{O}_3$ superlattices are strongly influenced by the depolarization field induced by the presence of the non-polar SrTiO_3 layers.²³ Compared to $\text{PbTiO}_3/\text{PbZr}_{0.2}\text{Ti}_{0.8}\text{O}_3$ superlattices, the addition of just two unit cells of SrTiO_3 at each interface changes the domain structure from 90° ferroelastic domains to 180° stripe nanodomains. This example illustrates the crucial role played by the electrostatic energy in stabilizing different polarization states in such ferroelectric heterostructures. Likewise, unexpected polarization enhancement was observed in $\text{SrTiO}_3/\text{BaTiO}_3/\text{CaTiO}_3$ superlattices.²⁴ Compared to BaTiO_3 alone, the presence of dielectric SrTiO_3 and CaTiO_3 layers in the tricolor superlattices enhanced the polarization, an effect ascribed to the interplay of compressive strain and depolarization fields. Additionally, studies of $\text{BaTiO}_3/\text{SrTiO}_3$ superlattices utilized the large strain between the materials to increase the dielectric constant by orders of magnitude compared to simple solid solutions.²⁵ These studies demonstrated how modern synthesis techniques can be applied to manipulate the elastic and electrostatic energies of a ferroelectric system and, in turn, they pave the way for future studies in which these effects could be used to stabilize unconventional ferroelectric structures.

Amongst ferroelectric heterostructures, however, there is one system that has proven to exhibit a rich variety of physical phenomena—that is, heterostructures and superlattices of PbTiO_3 and SrTiO_3 . In the bulk, PbTiO_3 has a tetragonal structure with a $P4mm$ space group and lattice parameters $a = 3.904 \text{ \AA}$ and $c = 4.178 \text{ \AA}$. PbTiO_3 is also a ferroelectric at room temperature with an axis of spontaneous polarization along the c axis ([001]) and undergoes a phase transition²⁶ from a tetragonal (ferroelectric) to a cubic (paraelectric) structure at $\sim 490^\circ\text{C}$. By contrast, SrTiO_3 is a band insulator at room temperature with a cubic structure with a $Pm3m$ space group and a lattice parameter $a = 3.905 \text{ \AA}$. Although SrTiO_3 is not polar at room temperature, it does undergo an interesting evolution at low temperatures in that it is an incipient ferroelectric which exhibits a quantum paraelectric phase, which is characterized by increasing permittivity with cooling as the lowest frequency polar optical phonon softens.²⁷ Leveraging advances in layer-by-layer growth, the similar in-plane lattice parameters and chemical framework, as well as the interesting polar or nearly polar nature of PbTiO_3 and SrTiO_3 , respectively, this system is a nearly ideal one for studying exotic effects in superlattices. In turn, ordered nano-domains with enhanced electrical properties and local structural distortions have been observed in short-period $\text{PbTiO}_3/\text{SrTiO}_3$ superlattices (i.e., superlattices with PbTiO_3 and SrTiO_3 layers ≤ 3 unit cells).^{28–31} Of particular importance was the observation of the so-called *improper ferroelectricity*, which arises due to antiferrodistortive/ferroelectric coupling and resulting interfacial oxygen octahedra rotations in short-period $(\text{PbTiO}_3)_n/(\text{SrTiO}_3)_m$ ($n < 9$, $m < 5$ unit cells)

superlattices.^{32–34} Whereas a conventional ferroelectric transition is characterized by the emergence of a net polarization, the phase transition of an improper ferroelectric has a different order parameter (e.g., the onset of octahedral rotations), and the electric polarization is a secondary effect. Because of this, improper ferroelectrics couple differently with electric fields and have a dielectric constant that is largely temperature independent, which is desirable for many technological applications. The existence of improper ferroelectricity in $\text{PbTiO}_3/\text{SrTiO}_3$ superlattices demonstrated a new method of interface engineering that can be used to manipulate material properties. It has also been shown in $(\text{PbTiO}_3)_5/(\text{SrTiO}_3)_n$ superlattices that PbTiO_3 has a negative dielectric constant in the temperature range of 420–700 K.³⁵ Devices using this “negative capacitance” effect could surpass the theoretical lower limit for power dissipation in conventional field-effect transistors.³⁶ At relatively large length scales (n and $m > 20$ unit cells), these superlattices form flux-closure polar domain patterns in order to reduce the depolarization field, producing a domain structure more reminiscent of a magnetic material than a ferroelectric.^{37,38}

At the same time, theoretical studies predicted that at intermediate length scales (n and $m = 10$ –20 unit cells), such superlattices could potentially support the formation of exotic topological structures including vortices and skyrmions as a result of the competition of different energies (i.e., elastic, electrostatic, and gradient).^{39–42} For example, in zero-dimensional $\text{PbZr}_{0.5}\text{Ti}_{0.5}\text{O}_3$ nanostructures, *ab initio* simulations predicted a phase transition that leads to the formation of a spontaneous toroidal moment in each (001); a structure that is characterized by a vortex-like configuration of electric dipoles.³⁹ This transition is driven by the finite size of the nanostructures and the strong depolarization fields that occur at their surfaces. Importantly, if such structures could be controlled and utilized in non-volatile ferroelectric memory devices, storage capacities could be orders of magnitude higher than devices using bulk ferroelectrics. Furthermore, similar vortex structures possessing a toroidal moment were predicted to form in $\text{PbTiO}_3/\text{SrTiO}_3$ superlattices.³¹ It was also predicted that geometric frustration in compositionally graded ferroelectrics could create exotic orderings such as stripe phases that give rise to interesting features such as a spiral state and topological defects.⁴⁰ In parallel, it was also predicted⁴³ that appropriate confinement of the material could drive the formation of electric skyrmion-like topologies in BaTiO_3 nanocomposites. All told, these studies demonstrate that careful control of material heterostructures and the local competition of energies can provide a pathway by which to manipulate the structural, polar, and physical nature of the mesoscale structures that emerge.

In this spirit, the recent discovery of polar-vortex structures in $(\text{PbTiO}_3)_n/(\text{SrTiO}_3)_n$ ($n = 10$ –20 unit cells)⁴⁴ superlattices is yet another example of an emergent phenomenon that can be stabilized by leveraging the interfacial effects of superlattice structures. In the following sections, we summarize past studies on nanoscale ferroelectrics and topologically protected structures (A brief history of exotic ferroelectric order); we then explore recent work on polar vortices including developing an understanding of the basic structure and energetics of formation (Polar vortices in $\text{PbTiO}_3/\text{SrTiO}_3$ superlattices), the observation of coexistence with ferroelectric domains (Toroidal order and coexistence with ferroelectric order), observations of cross-coupling of electric and toroidal-order parameters (Electric-field control of toroidal-vortex and ferroelectric order), and chirality (Chirality in polar vortices). We end by briefly looking to the future for what might be possible in these systems in the years to come (Looking to the future).

A BRIEF HISTORY OF EXOTIC FERROELECTRIC ORDER

Ferroelectricity and ferromagnetism are two phenomena that are of fundamental interest and technological importance. Ferroelectric and ferromagnetic materials both evolve from their respective paraelectric and paramagnetic parent phases as their temperature is lowered below the Curie temperature. In each case, the characteristic order parameter of the transition is the spontaneous formation of a net electric or magnetic polarization (i.e., a collective ordering of electric or magnetic dipoles). Although they were not described theoretically by Weiss until 1905,⁴⁵ ferromagnets were discovered centuries ago and fascinated scientists due to their ability to exert forces at a distance and for their use in magnetic compasses. By contrast, the word “ferroelectric” did not even exist until 1912 when Debye,⁴⁶ by analogy to ferromagnetism, provided the first theoretical description of ferroelectricity and the first observation of spontaneous electrical polarization in ferroelectric Rochelle

salt was in 1920.⁴⁷ Since that time, however, understanding and utilization of both materials have progressed at a rapid pace, and today both ferroelectrics (e.g., in sonar, actuator/transducer, ultrasonic devices) and ferromagnets (e.g., in data storage, magnetic cores, motors) are used widely.

Although these two ferroic orders are each defined by the spontaneous alignment of dipoles, the mechanisms that drive these collective phenomena are quite different. In ferromagnets, there must first be unpaired electrons such that the net spin is non-zero. If unpaired electrons are present, their ordering is driven by the competition between exchange interaction and thermal energy. Dictated by quantum mechanical symmetry restrictions, the exchange interaction in a ferromagnet is minimized when electron spins align, creating a net macroscopic, observable magnetization. In ferroelectrics, on the other hand, there must first be an offset of positive and negative ions (i.e., formation of an electric dipole) in order to have a polarization. In most ferroelectrics, this occurs due to a symmetry-lowering distortion that minimizes the energy of filled atomic orbitals, known as a second-order Jahn-Teller effect.⁴⁸ Once the electric dipoles are present, their long-range ordering is stabilized by dipole-dipole interactions, leading to a net macroscopic and observable electric polarization.

Ferroic materials also have a tendency to form domains—or local regions of uniform polarization/magnetization—as a means to reduce the depolarization/demagnetization fields that occur at surfaces. Although uniform domains wherein polarization/magnetization are locally aligned in a parallel fashion are by far the most common arrangement, there is considerable interest in the potential for more exotic, smoothly varying dipole topologies to form in both ferroelectrics and ferromagnets. In magnetic systems, the existence of vortex-like states is well documented. As far back as the 1940s, Kittel proposed that depending on the exchange interaction and crystallographic anisotropy energies, different magnetization patterns are possible in magnetic materials.⁴⁹ Ring- or vortex-like structures are predicted when exchange interactions between adjacent magnetic moments dominate over anisotropy [Fig. 1(a)], and flux-closure structures will develop when the anisotropy energy dominates [Figs. 1(b) and 1(c)]. Such domain arrangements are common in magnetic materials, in particular, when they are reduced to small sizes. As such, experimental observations of flux-closure domains^{50–53} and vortices^{54–56} are well documented. More complex topological patterns [Figs. 1(d)–1(f)] can develop depending on the relative strengths of the exchange, crystallographic anisotropy, and demagnetization energies in magnetic systems.^{57,58} The resulting complicated

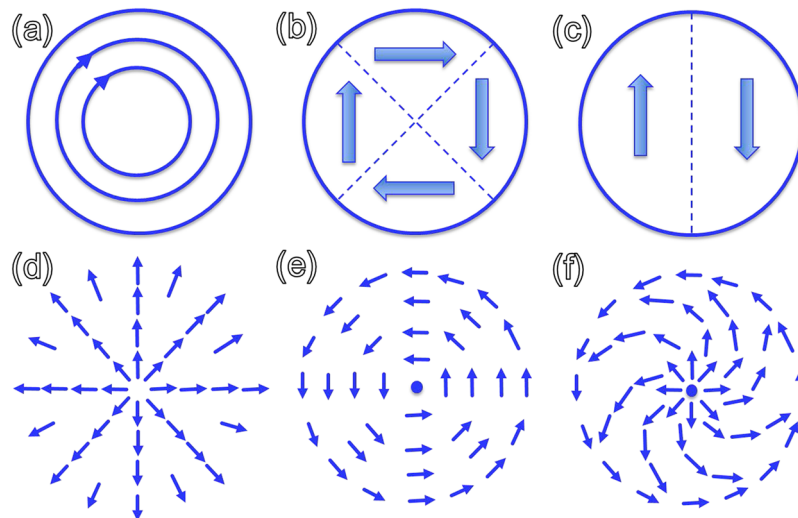


FIG. 1. Kittel proposed⁴⁹ different types of magnetic domain arrangements including (a) ring/vortex-like patterns, which apply for materials with low anisotropy, (b) flux-closure patterns for materials with high anisotropy (and cubic symmetry), and (c) two domains, with the magnetization in opposite directions in each domain for high anisotropy in a uniaxial crystal. In turn, Mermin also described a number of [(d), (e), and (f)] complex topological patterns that could be possible in ferroic systems.⁵⁷ Reprinted with permission from Kittel, *Rev. Mod. Phys.* **21**, 541 (1949). Copyright 1949 American Physical Society. Reprinted with permission from Mermin, *Rev. Mod. Phys.* **51**, 591 (1979). Copyright 1979 American Physical Society.

patterns involving spirals of continuously rotating magnetic dipoles have been observed, most notably in magnetic skyrmions.^{59,60}

In analogy to magnetic materials, the discussion of domain structures and topologies in ferroelectrics began in the early 2000s. Initial interest was prompted by the desire to understand the behavior of low-dimensional ferroelectrics. Studies on thin (<50 nm thick) PbTiO₃ films showed the existence of nanoscale 180° stripe domains, resembling the uniform domains observed in bulk PbTiO₃.⁶¹ Furthermore, it was shown that ferroelectricity can exist in PbTiO₃ films as thin as just three unit cells.⁶² These studies on ultrathin PbTiO₃, however, left open the question of how manipulating a single-layer system (e.g., by adding dielectric or conducting layers to affect electrostatic boundary conditions) could change the ferroelectric properties. Theoretical studies of low-dimensional ferroelectric nanostructures—such as in BaTiO₃,⁶³ Pb(Zr_{0.5}Ti_{0.5})O₃,³⁹ and PbTiO₃⁶⁴—suggested the potential to form new electric dipole arrangements characterized by the spontaneous formation of a toroidal moment. The toroidal moment, which is nonzero for a curling configuration of electric dipoles, was predicted to appear in low-dimensional structures where strong depolarizing fields prevent the formation of uniform domains. Today, the search is still ongoing to find such complex dipole structures in ferroelectrics and multiferroics.^{58,65} As in ferromagnets, it was shown experimentally that flux-closure domains can occur in ferroelectrics by exploiting the right combination of reduced dimensionality, strain, and electrostatic energies.³⁷ Such flux-closure domains in ferroelectrics were first observed in PbZr_{0.2}Ti_{0.8}O₃ layers.⁶⁶ Despite this interest, it would take over a decade for experimentalists to realize for the first time the direct observation of such smoothly rotating polar structures. In the end, such structures were realized, not in nanostructured ferroelectrics in a paraelectric matrix, but in (PbTiO₃)_n/(SrTiO₃)_n superlattices where polar vortices were observed in 2016.⁴⁴ This observation pushed the community to question its assumptions about what is possible in these systems and immediately begs the question as to whether more complex topological structures can be stabilized in ferroelectrics? In turn, much discussion has been focused on whether or not the electrical equivalent of a skyrmion exists,^{43,58} but the experimental investigations into electric topological configurations are just beginning.

POLAR VORTICES IN PbTiO₃/SrTiO₃ SUPERLATTICES

Leveraging advances in advanced atomic-resolution electron microscopy, researchers were able to produce a vector map of the atomic-polar displacements (P_{PD})^{44,67} from a cross-sectional high-resolution scanning transmission electron microscopy (HR-STEM) image for a (PbTiO₃)₁₀/(SrTiO₃)₁₀ superlattice [Fig. 2(a)]. Such real-space images of polar structure revealed the formation of a long-range array of left- and right-handed vortex pairs in each PbTiO₃ layer. Close inspection of a single vortex pair [Fig. 2(b)] shows the continuous rotation of the polarization state within the lattice. The lateral periodicity of these vortex pairs (i.e., from one right-handed to the next right-handed vortex) was found to be ~10 nm and to scale with the thickness of the PbTiO₃ layers in the superlattices. Low-resolution, cross-sectional dark-field transmission electron microscopy (DF-TEM) imaging [Fig. 2(c)], in turn, revealed a pseudo-long-range periodic array of intensity modulations along both in- and out-of-plane directions of the superlattice, corresponding to the vortex pairs with a spacing of ~10 nm. In such images, each bright/dark contrast modulation corresponds to one vortex pair. Upon rotating the sample and looking down at the surface of the superlattice structure, plan-view DF-TEM images [Fig. 2(d)] revealed long-range ordered arrays of stripe contrast with a lateral periodicity of ~10 nm, suggesting that the polar vortices extend through the film over many hundreds of nanometers length scale. Again, this observation of arrays of polar vortices represents the first experimental realization of such structures and the identification of a novel state of matter.

To understand why such vortex structures formed, phase-field modeling was used to probe the polarization structure according to the time-dependent Ginzburg-Landau equation (detailed methods in Ref. 43). Ultimately, the phase-field models were able to replicate the 3D structure of the vortex array (Fig. 3). The models revealed that neighboring vortices indeed have opposite signs for the curl of the polarization (matching that observed from the experiments) and that the vortices form long, tube-like features that extend along the in-plane direction of the film. More importantly, the phase-field simulations shed light on the energies at play in the formation of these emergent features. Ultimately, it

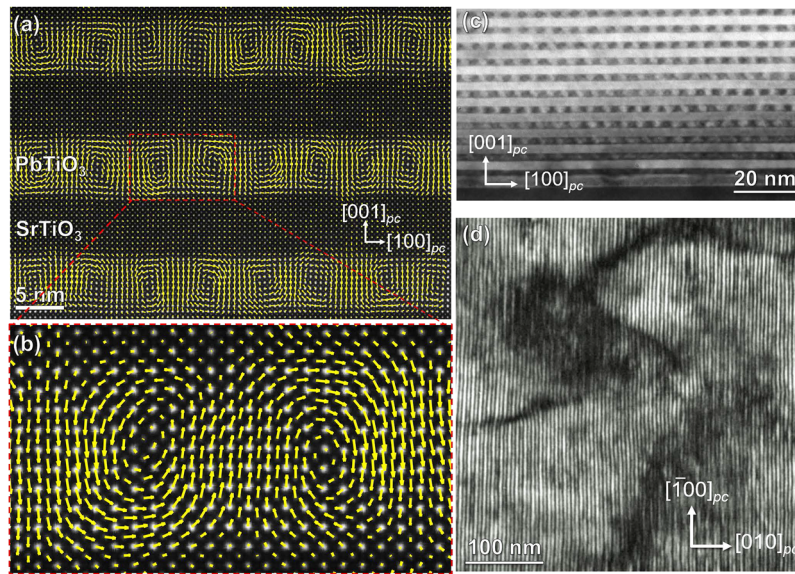


FIG. 2. (a) Cross-sectional HR-STEM image with mapping of the titanium-ion displacement vectors (\mathbf{P}_{PD} , indicated by yellow arrows) for an $n = 10$ superlattice, revealing a quasi-ordered array of left- and right-handed vortices in pairs in each PbTiO_3 layer. (b) A magnified image of a single vortex pair showing the smoothly varying polarization. (c) Cross-sectional DF-TEM image of an $n = 10$ superlattice showing the long-range ordering of vortices; each light-dark contrast change is a vortex pair. (d) Planar-view DF-TEM image of an $n = 16$ superlattice, which exhibits long-range in-plane ordering associated with the vortex pairs. Reprinted with permission from Yadav *et al.*, Nature **530**, 198 (2016). Copyright 2016 Springer Nature.

was determined that the vortex structures arise from a competition between three energies: (1) elastic energy—the PbTiO_3 layers are under tensile strain when grown on the $\text{DyScO}_3 (110)_o$ substrates. This epitaxial constraint favors the formation of c/a domain structures wherein there is a mixture

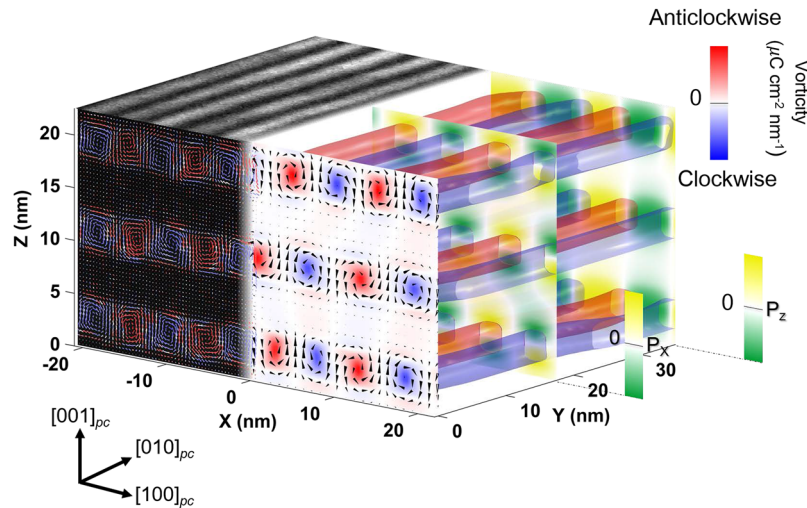


FIG. 3. Three-dimensional representation showing both the cross section and plan-view HR-STEM data from the experiment (left) compared with the optimized phase-field simulations (right) for an $n = 10$ superlattice. The front cross section of the phase-field model shows the polarization vector \mathbf{P} ordered into clockwise (blue) and anticlockwise (red) vortex states, which extend along the $[010]_{pc}$. For comparison, on the left is shown a cross-sectional HR-STEM image overlaid with a polar displacement vector map and a planar-view DF-TEM image projected onto the front and top planes of the axes, respectively. Red/blue color scales correspond to the curl of the polarization extracted from the phase-field model and the HR-STEM polar displacement map (\mathbf{P}_{PD}). The scale bars on P_x and P_z are from -44.81 to 44.81 ($\mu\text{C cm}^{-2}$) and from -54.24 to 54.24 ($\mu\text{C cm}^{-2}$), respectively, whereas the vorticity is from -129.36 to 129.36 ($\mu\text{C cm}^{-2} \text{ nm}^{-1}$). Reprinted with permission from Yadav *et al.*, Nature **530**, 198 (2016). Copyright 2016 Springer Nature.

of out-of-plane polarized c and in-plane polarized a domains. (2) Electrostatic energy—at the same time, there is a polar discontinuity at the $\text{PbTiO}_3/\text{SrTiO}_3$ interface, which is a driving force for the formation of bound charges (or built-in fields) as the gradient of the polarization is not equal to zero. (3) Gradient energy—this is a measure of the cost for polarization rotation in the material. Overall, the presence of the polar PbTiO_3 layers, sandwiched between the dielectric SrTiO_3 layers, leads to an effective frustration or competition that drives the system to a new instability and the formation of a novel polarization topology.

TOROIDAL ORDER AND COEXISTENCE WITH FERROELECTRIC ORDER

Building from the initial observation and understanding of the nature of the vortex structures, subsequent studies on the evolution of the $(\text{PbTiO}_3)_n/(\text{SrTiO}_3)_n$ superlattices with period n revealed a number of important observations. First, for short-period superlattices ($n = 4\text{--}10$ unit cells), structures consistent with traditional ferroelectric domain structures (so-called a_1/a_2 domain patterns) with fully in-plane oriented polarization were observed. This was evident from both piezoresponse force microscopy and synchrotron-based 3D reciprocal space mapping (RSM) studies. For example, for an $n = 6$ superlattice, such RSM studies about the pseudocubic 002 -diffraction condition of the DyScO_3 substrate [Fig. 4(a)] reveal regular peaks along the out-of-plane (Q_z) direction, corresponding to the out-of-plane periodicity of the superlattice. No peaks are observed in the in-plane (Q_x or Q_y) directions, demonstrating the lack of domains with out-of-plane polarization components. Further RSM studies about the pseudocubic 202 -diffraction condition of the DyScO_3 substrate [Fig. 4(b)] are sensitive to modulations of in-plane polarization, and strong satellite peaks are observed along the in-plane directions due to the formation of periodic ferroelectric a_1/a_2 domains of periodicity ~ 70 nm

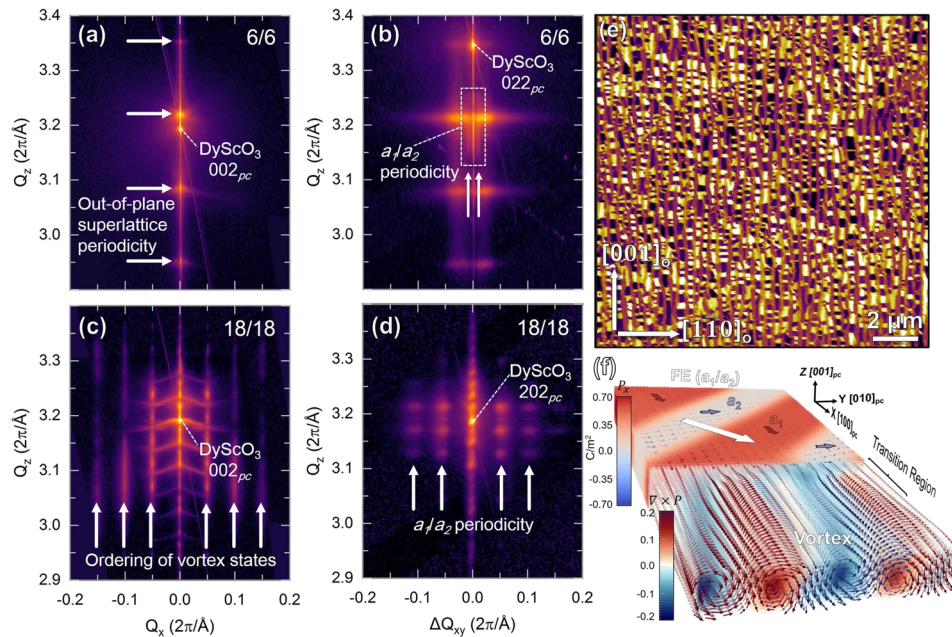


FIG. 4. Reciprocal space mapping (RSM) studies for an $n = 6$ superlattice about the (a) 002_{pc} -diffraction peak of the DyScO_3 substrate revealing no satellite peaks present along the in-plane (Q_x) direction, indicating that the vortex phase is not present, and (b) 202_{pc} -diffraction peak of the DyScO_3 substrate revealing satellite peaks that run along the in-plane $[110]_{pc}$, indicative of the presence of a_1/a_2 domains. RSM studies for an $n = 18$ superlattice about the (c) 002_{pc} -diffraction peak of the DyScO_3 substrate revealing satellite peaks along the in-plane (Q_x) direction, corresponding to the ordering of the vortex states, and (d) 022_{pc} -diffraction peak of the DyScO_3 substrate revealing satellite peaks along the in-plane $[110]_{pc}$, indicating that a_1/a_2 domains are also present. (e) Piezoresponse force microscopy image showing macroscopic ordering of the two phases in an $n = 16$ superlattice. Alternating brown and black/white checkboard stripes correspond to alternating regions of low and high piezoresponse (i.e., regions of vortex and a_1/a_2 domains, respectively). (f) Phase-field modeling also predicts the mixed-phase (vortex and a_1/a_2) structure. The curl of the polarization in the vortices is represented by the red/blue coloring. Reprinted with permission from Damodaran *et al.*, Nat. Mater. **16**, 1003 (2017). Copyright 2017 Springer Nature.

with domain walls along the pseudocubic [110]. On transitioning to intermediate period superlattices ($n = 12-18$), however, more complex RSM studies are observed showing the presence of both the ferroelectric a_1/a_2 phase and peaks for a new phase. For example, for an $n = 18$ superlattice, RSM studies about the pseudocubic 002-diffraction condition of the DyScO₃ substrate [Fig. 4(c)] reveal the presence of satellite peaks along the in-plane (Q_x) direction. This is indicative of a periodic modulation of the out-of-plane component of polarization along the in-plane direction and corresponds to features with a periodicity of ~ 12.5 nm—the same as that expected for the vortex pairs in this superlattice. At the same time, however, and similar to the $n = 6$ superlattice, off-axis RSM studies about the pseudocubic 220-diffraction condition of the DyScO₃ substrate [Fig. 4(d)] reveal satellite peaks along the in-plane directions indicative of ferroelectric a_1/a_2 domains with a periodicity of ~ 12 nm.

This coexistence of a classic ferroelectric and the new, emergent vortex phase can be nicely visualized using piezoresponse force microscopy [Fig. 4(e)].⁶⁸ The resulting self-assembled, hierarchical structure reveals stripe-like order in which alternating stripes exhibit high (checkered white and black) and low or zero (brown) piezoresponse with a periodicity of ~ 300 nm along the in-plane pseudocubic [100]. The high-response regions are the ferroelectric a_1/a_2 phase, and the low-response regions are the vortex structures. Ultimately, these data indicate that at room temperature, the coexisting vortex and ferroelectric phases spontaneously assemble in a mesoscale, fiber-textured, hierarchical superstructure. Such a structure was also replicated in large-scale phase-field models. For example, the evolution of a single PbTiO₃ layer within the superlattice near the phase boundary between the ferroelectric and vortex phases can be extracted for close inspection [Fig. 4(f)]. Such an approach allows one to track the evolution of the polarization across the boundary between the ferroelectric and vortex phases. Surprisingly, it was found that the polarization component along the length of the vortex tube does not go to zero. This was confirmed by piezoresponse force microscopy studies which showed the presence of in-plane polarization in the vortex phase. This means that the vortices are not just tubes of wrapped polarization (like a rolled-up piece of paper) but are more like a spiral with an axial component of polarization. It has been predicted for some time that polarization waves, vortices, etc., could be characterized by an emergent order parameter, a so-called electric toroidal moment $\mathbf{G} = \frac{1}{2V} \int \mathbf{r} \times \mathbf{P}(\mathbf{r}) d^3r$.^{39,69,70} Such toroidal moments can give rise to a range of novel phenomena, including pyrotoroidic, piezotoroidic, and other effects. Extraction of \mathbf{G} from these vortex structures revealed that there is a non-zero electric toroidal moment that ultimately saturates to values of $0.2e \text{ \AA}^{-1}$ and arises from the screw-like character of polarization in the vortex phase and suggests that the superlattice structures are characterized by a multiorder-parameter state consisting of axial ferroelectric polarization that coexists with \mathbf{G} . Such 3D polarization texture, in turn, presents intriguing possibilities for another emergent function, including chirality, which will be discussed in the section titled Chirality in polar vortices.

ELECTRIC-FIELD CONTROL OF TOROIDAL-VORTEX AND FERROELECTRIC ORDER

The presence of the axial component of polarization had other important implications—namely that with this axial polarization component, dc electric field manipulation of the vortex phase could be possible. To probe this concept, researchers explored the evolution of the mixed-phase ferroelectric/vortex structures under applied dc electric fields using piezoresponse force microscopy.⁶⁸ For example, the as-grown mixed-phase structure for an $n = 16$ superlattice again reveals the spontaneously assembled mesoscale, fiber-textured, hierarchical superstructure for ferroelectric and vortex regions [Fig. 5(a)]. Upon application of a positive dc bias to a specific area of the sample [orange box, Fig. 5(a)], however, the mixed-phase structure is transformed into a pure vortex phase with uniformly low piezoresponse [Fig. 5(b)]. This transition was also confirmed via nanoscale X-ray diffraction experiments. The resulting pure vortex phase can, in turn, be switched back to have a mixture of ferroelectric and vortex phases with application of a negative dc bias [Fig. 5(c)]. Close inspection, however, reveals that directly under the tip where the bias was applied, the sample remains within the low piezoelectric response vortex phase, indicating that the vortex phase persists [blue arrows, Fig. 5(c)], but in adjacent regions where the applied bias from the scanning probe tip has a significant in-plane field component, high piezoelectric response ferroelectric structures with in-plane polarization are produced. Additionally, it should be noted that reversing the applied field (i.e., a

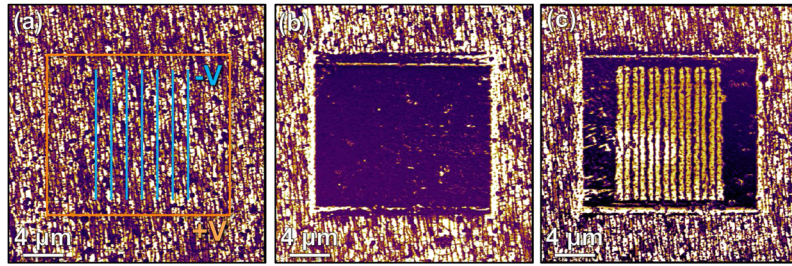


FIG. 5. (a) Piezoresponse force microscopy (lateral amplitude) images for an $n = 16$ superlattice showing mixed-phase structure in the as-grown condition. (b) Upon application of a positive voltage in the orange box of (a), the material transforms to a uniformly low-piezoresponse vortex phase. (c) Subsequent application of a negative bias to the blue lines of (b) results in the creation of ferroelectric phases and the recovery of a mixed-phase structure. Reprinted with permission from Damodaran *et al.*, *Nat. Mater.* **16**, 1003 (2017). Copyright 2017 Springer Nature.

negative followed by a positive bias) produces similar effects. This reversible electric-field control of ferroelectric and electric toroidal order provides for a number of novel opportunities for applications. For example, regions of pure vortex order exhibit order-of-magnitude lower piezoresponse and non-linear optical effects; indicating that one can electrically manipulate and dramatically change materials properties.⁶⁸ The ability to write vortex regions and control the toroidal order with an applied electric field suggests a coupling between the toroidal and ferroelectric order parameters that can be exploited to control other materials properties—namely, the chirality. Electric control of the chirality and other coupled properties would open a new frontier in condensed matter physics and building multi-functional devices.

CHIRALITY IN POLAR VORTICES

Based on the observation of an axial component of polarization in the toroidal polar vortices, the intriguing possibility of chirality was explored. Chirality is a geometrical property by which an object is not superimposable onto its mirror image, thereby imparting a handedness. In condensed-matter physics, the prediction of topologically protected magnetic skyrmions and related spin textures in chiral magnets draws parallels to the polar vortex structures observed herein and begs the question that if the magnetic dipoles were replaced by their electrical counterparts, then could we realize electrically controllable chiral devices? In turn, using resonant soft X-ray diffraction (RSXD) experiments [Fig. 6(a)], researchers indeed proved the chiral nature of these materials.⁷¹ In the RSXD

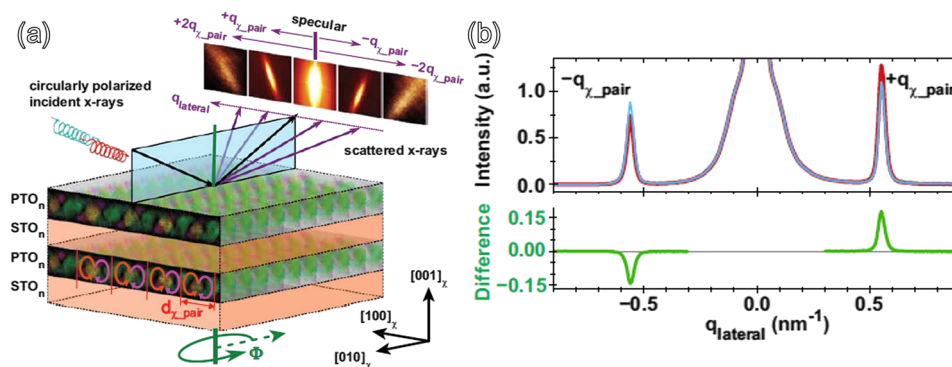


FIG. 6. (a) Schematic illustrating the experimental setup for the RSXD studies. The data on the top right are actual images of the specular beam and various higher-order satellite peaks that can be observed. (b) The top panel shows a line-cut of the scattered intensity versus lateral momentum transfer using right- (red) and left-circularly (blue) polarized X-rays for an $n = 16$ superlattice. The lower panel shows the difference in intensity between the two helicities and that there is a significant dichroism at the vortex peaks, indicative of the chiral nature of the polar vortex phase. Reprinted with permission from Shafer *et al.*, *Proc. Nat. Acad. Sci. U. S. A.* **115**, 915 (2018). Copyright 2018 National Academy of Sciences.

setup, the superlattices were aligned so that the incoming X-rays were incident parallel to the axes of the vortices. A specular spot was observed, corresponding to diffraction from the out-of-plane ordering of the superlattice structure. Similar to the RSM studies [Fig. 4(c)], lateral satellites appear due to the regular spacing of the vortex structures. By tuning the energy of the X-rays through the titanium $L_{3,2}$ edge (where electronic transitions from the $2p$ to $3d$ orbitals occur), energy spectra were collected for the satellite peaks. In particular, the X-ray circular dichroism at these peaks was probed. At the titanium $L_{3,2}$ resonances, effects from the electronic structure (specifically, the d orbital configuration) are strongly enhanced. If the spiraling polar distortions that create the vortex phase are chiral, this will manifest as a non-zero circular dichroism since chiral objects interact differently with left- and right-circularly polarized light. The intensity of diffraction for right- (red) and left-circularly (blue) polarized light as a function of Q_x is shown [Fig. 6(b)], along with the X-ray circular dichroism [XCD; bottom, Fig. 6(b)], which is the difference between the scattered intensity for right- and left-circularly polarized light. The presence of dichroism is indicative of a chiral structure, as is the anti-symmetric nature of the dichroism signal as the q vector is reversed from positive to negative.

LOOKING TO THE FUTURE

The recent discovery of emergent phenomena in $\text{PbTiO}_3/\text{SrTiO}_3$ superlattices—namely, the novel chiral polar vortices and their associated complex phase coexistence and response under applied fields—suggests the presence of a complex, multi-dimensional system capable of exotic function. The first, and potentially most important, question is how far can the analogy with magnetic spin topologies be taken? Can continued evolution of the growth and control of the $\text{PbTiO}_3/\text{SrTiO}_3$ system (or related systems) enable researchers to generate true electronic skyrmions which can be rigorously and mathematically defined akin to their magnetic brethren? Do such vortex structures have to coexist with ferroelectric order or can we realize pathways to creating fully vortex structures? Are there other emergent polarization topologies possible in these structures? Such questions and their ultimate realization will require considerable advances in both experimental synthesis and characterization, and computational and modeling approaches to explore this complex, diverse landscape. Along these lines, there are likely numerous routes which can be pursued in an attempt to realize other novel topologies and phenomena. Focusing first on additional ferroelectric phenomena, the study of $\text{PbTiO}_3/\text{SrTiO}_3$ superlattices is far from complete, and studies wherein either the substrate (i.e., the strain state) or the dielectric buffer layer is replaced with other materials seem warranted. Such approaches are motivated by the fact that epitaxial constraints can have a marked and predictable impact on the evolution of polarization from more out-of-plane to in-plane tendency, thus providing an additional knob to manipulate the nature of the emergent structures. By varying the dielectric buffer layer, one can control aspects like the elastic stiffness/compliance and dielectric constant, which will again work to tip the balance of the energy scales in a manner that could drive further exotic structures to form. From there, the exploration of asymmetric superlattices (wherein the thickness of the nearest SrTiO_3 and/or PbTiO_3 layers is varied in a periodic manner) or even “tricolor” superlattices (of the form $A/B/C/A/B/C$) could provide a route to break the out-of-plane symmetry of the structures and drive a new function. There are even potential concepts beyond ferroelectrics, where similar competition of energies in magnetic or multiferroic systems could be of interest. For example, superlattices based on similar diamagnetic/ferromagnetic and dielectric-diamagnetic/multiferroic building blocks could give rise a pathway to the development of emergent spin or multi-order polarization/spin structures. In the end, observation of such features and discovery of new features would effectively fulfill years of predictions and rewrite some of our fundamental assumptions about what is possible in these materials.

At the same time, we have only just begun to scratch the surface of our understanding of these emergent features. The few initial studies have already demonstrated interesting and important points—specifically, electric-field control and interconversion between classical ferroelectric and emergent vortex structures, the realization of electric-toroidal order, and emergent chirality in a ferroelectric-based system. What are the prospects for using the electric-field control to generate new applications (e.g., tuning states in memory or logic and manipulating electro-optic effects)? The emergence of electric toroidal order implies the potential to probe new effects such as pyrotoroidic and

piezotoroidic effects, which have long been proposed but not fully realized. Likewise, the prospect for controllable chirality with an electric field is an intriguing dream. Can we design an approach that allows for manipulation of the polar structures in a deterministic manner that changes, for example, handedness of the features with a homogeneous dc electric field? The ability to switch chirality with homogenous magnetic fields⁷² or ac electric currents⁷³ has been demonstrated for magnetic structures, and switching by electric fields is possible with, for example, the addition of voltage-induced strain.⁷⁴ In polar vortex structures, their chiral nature⁷¹ and toroidal coupling to electric fields⁶⁸ have already been established, and attempts to utilize this coupling to achieve electric-field control seem to merit deeper consideration.

There is also considerable potential for novel dynamics in these complex polarization structures. To date, there has been no study of the dynamics and evolution of these emergent features in either equilibrium or non-equilibrium (i.e., driven) conditions. In classical ferroelectrics, years of research have provided an understanding of switching processes (including aspects of nucleation and growth of domains) as well as the ultra-fast dynamics within the unit cell. Numerous studies today probe how ferroelectrics respond under electric field or light excitation and glean insights into how polarization evolves and novel states that can be accessed. The complex, mesoscale structure of the emergent vortex and related states are sure to exhibit effects fundamentally different from those of the individual parent materials. The long-range structures suggest the potential for soft, low-frequency, and non-traditional temperature and field dependence. The effect of such emergent polarization structures on photo-excited charges could be dramatically different from those in a homogenous polarization state. As such, studies of fluctuations, both in equilibrium and non-equilibrium conditions, and structural and polar dynamics under excitation are ripe for exploration. Effects like the bulk photovoltaic effect and how this will be altered in these inhomogeneous polarization profiles could lead to exotic charge dynamics and effects, all of which remain to be probed.

Finally, it cannot be overlooked that these observations of emergent features can potentially lead to new manifestations of applications. Besides gaining important fundamental knowledge about these new polar structures, researching and understanding vortices can lead to new technological applications, such as non-volatile memory devices or an electric analog to a “racetrack memory.”^{75,76} The intriguing potential for coupled effects between light and polarization could also lead to new modalities of data storage and retrieval based on light. Moving forward, these prospects may inspire new mechanisms through which the deterministic writing and reading of nanoscale chiral structures can be achieved. What is clear is that we are only at the beginning of our work to understand, control, and ultimately utilize these exciting emergent structures in polar materials.

ACKNOWLEDGMENTS

The authors acknowledge support of the Gordon and Betty Moore Foundation’s EPiQS Initiative, under Grant No. GBMF5307, the Army Research Office, under Grant No. W911NF-14-1-0104, the National Science Foundation, under Grant Nos. DMR-1451219, CMMI-1434147, DMR-1608938, OISE-1545907, and DMR-1708615, the National Science Foundation Graduate Research Fellowship, under Grant No. DGE-1106400, the U.S. Department of Energy, Office of Science, Office of Basic Energy Sciences, Materials Sciences and Engineering Division, under Contract No. DE-AC02-05-CH11231: Materials Project program KC23MP, and the Office of Basic Energy Sciences, under Award No. DE-SC-0012375. Use of the Advanced Photon Source was supported by the U.S. Department of Energy, Office of Science, Office of Basic Energy Sciences, under Contract No. DE-AC02-06CH11357. This research used resources of the Advanced Light Source, which is a DOE Office of Science User Facility under Contract No. DE-AC02-05CH11231. Work at the Molecular Foundry was supported by the Office of Science, Office of Basic Energy Sciences, of the U.S. Department of Energy under Contract No. DE-AC02-05CH11231.

¹ H. Y. Hwang *et al.*, *Nat. Mater.* **11**, 103 (2012).

² J. Mannhart and D. G. Schlom, *Science* **327**, 1607 (2010).

³ M. Stengel *et al.*, *Nat. Mater.* **8**, 392 (2009).

⁴ A. Ohtomo and H. Y. Hwang, *Nature* **427**, 423 (2004).

⁵ N. Reyren, S. Thiel, A. D. Caviglia, L. Fitting Kourkoutis, G. Hammerl, C. Richter, C. W. Schneider, T. Kopp, A.-S. Rüetschi, D. Jaccard, M. Gabay, D. A. Müller, J.-M. Triscone, and J. Mannhart, *Science* **317**, 1196 (2007).

⁶ H. Song, T. Susaki, and H. Y. Hwang, *Adv. Mater.* **20**, 2528 (2008).

- ⁷ Y. Tokura, *Colossal Magnetoresistive Oxides* (Gordon and Breach Science Publishers, Amsterdam, 2000), Vol. 2.
- ⁸ D. G. Schlom *et al.*, *Annu. Rev. Mater. Res.* **37**, 589 (2007).
- ⁹ S. Das *et al.*, *Phys. Rev. B* **91**, 134405 (2015).
- ¹⁰ M. Ye. Zhuravlev, R. F. Sabirianov, S. S. Jaswal, and E. Y. Tsymbal, *Phys. Rev. Lett.* **94**, 246802 (2009).
- ¹¹ K. Ueda, H. Tabata, and T. Kawai, *Science* **280**, 1064 (1998).
- ¹² X. Ke, M. S. Rzchowski, L. J. Belenky, and C. B. Eom, *Appl. Phys. Lett.* **84**, 5458 (2004).
- ¹³ M. Gibert, P. Zubko, R. Scherwitzl, J. Íñiguez, and J.-M. Triscone, *Nat. Mater.* **11**, 195 (2012).
- ¹⁴ F. Nolting, A. Scholl, J. Stöhr, J. W. Seo, J. Fompeyrine, H. Siegwart, J.-P. Locquet, S. Anders, J. Lüning, E. E. Fullerton, M. F. Toney, M. R. Scheinfein, and H. A. Padmore, *Nature* **405**, 767 (2000).
- ¹⁵ M. Bibes, J. E. Villegas, and A. Barthélémy, *Adv. Phys.* **60**, 5 (2011).
- ¹⁶ Y.-H. Chu, L. W. Martin *et al.*, *Nat. Mater.* **7**, 478 (2008).
- ¹⁷ C.-G. Duan, S. S. Jaswal, and E. Y. Tsymbal, *Phys. Rev. Lett.* **97**, 047201 (2006).
- ¹⁸ X. Hong, A. Posadas, A. Lin, and C. H. Ahn, *Phys. Rev. B* **68**, 134415 (2003).
- ¹⁹ T. Lottermoser, T. Lonkai, U. Amann, D. Hohlwein, J. Ihringer, and M. Fiebig, *Nature* **430**, 541 (2004).
- ²⁰ D. Chiba, M. Yamanouchi, F. Matsukura, and H. Ohno, *Science* **301**, 943 (2003).
- ²¹ T. Kimura, T. Goto, H. Shintani, K. Ishizaka, T. Arima, and Y. Tokura, *Nature* **426**, 55 (2003).
- ²² M. Dawber, K. M. Rabe, and J. F. Scott, *Rev. Mod. Phys.* **77**, 1083 (2005).
- ²³ M. Lemée *et al.*, *ACS Appl. Mater. Interfaces* **7**, 19906 (2015).
- ²⁴ H. N. Lee *et al.*, *Nature* **433**, 395 (2005).
- ²⁵ H. Tabata, H. Tanaka, and T. Kawai, *Appl. Phys. Lett.* **65**(15), 1970 (1994).
- ²⁶ Y. Kuroiwa, S. Aoyagi, and A. Sawada, *Phys. Rev. Lett.* **87**, 217601 (2001).
- ²⁷ K. A. Muller and H. Burkard, *Phys. Rev. B* **19**, 3593 (1979).
- ²⁸ M. Dawber *et al.*, *Phys. Rev. Lett.* **95**, 177601 (2005).
- ²⁹ P. Zubko *et al.*, *Phys. Rev. Lett.* **104**, 187601 (2010).
- ³⁰ P. Zubko *et al.*, *Ferroelectrics* **433**, 127 (2012).
- ³¹ P. Zubko *et al.*, *Nano Lett.* **12**, 2846 (2012).
- ³² E. Bousquet, M. Dawber, N. Stucki, C. Lichtensteiger, P. Hermet, S. Gariglio, J.-M. Triscone, and P. Ghosez, *Nature* **452**, 732 (2008).
- ³³ D. Sichega *et al.*, *Phys. Rev. Lett.* **104**, 207603 (2010).
- ³⁴ J. H. Zhao *et al.*, *Phys. Rev. B* **89**, 174101(R) (2014).
- ³⁵ P. Zubko, J. C. Wojdeł, M. Hadjimichael, S. Fernandez-Pena, A. Sené, I. Luk'yanchuk, J.-M. Triscone, and J. Íñiguez, *Nature* **534**, 524 (2016).
- ³⁶ S. Salahuddin and S. Datta, *Nano Lett.* **8**, 405–410 (2008).
- ³⁷ Y. L. Tang, Y. L. Zhu *et al.*, *Science* **348**, 547 (2015).
- ³⁸ C. L. Jia *et al.*, *Science* **331**, 1420 (2011).
- ³⁹ I. I. Naumov, L. Bellaiche, and H. Fu, *Nature* **432**, 737–740 (2004).
- ⁴⁰ N. Choudhury, L. Walizer, S. Lisenkov, and L. Bellaiche, *Nature* **470**, 513 (2011).
- ⁴¹ S. Prosdandeev and L. Bellaiche, *Phys. Rev. B* **75**, 094102 (2007).
- ⁴² S. Prosdandeev *et al.*, *J. Phys. Condens. Matter* **20**, 193201 (2008).
- ⁴³ Y. Nahas, S. Prokhorenko, L. Louis, Z. Gui, I. Kornev, and L. Bellaiche, *Nat. Commun.* **6**, 8542 (2015).
- ⁴⁴ A. K. Yadav *et al.*, *Nature* **530**, 198 (2016).
- ⁴⁵ P. Weiss, *J. Phys.: Theor. Appl.* **6**, 661 (1907).
- ⁴⁶ P. Debye, *Z. Phys.* **13**, 97 (1912).
- ⁴⁷ J. Valasek, *Phys. Rev.* **17**, 475 (1921).
- ⁴⁸ J. B. Goodenough, *J. Phys. Chem. Solids* **25**, 151 (1964).
- ⁴⁹ C. Kittel, *Rev. Mod. Phys.* **21**, 541 (1949).
- ⁵⁰ R. D. Gomez, T. V. Luu, A. O. Pak, K. J. Kirk, and J. N. Chapman, *J. Appl. Phys.* **85**, 6163 (1999).
- ⁵¹ R. Pulwey, M. Zölff, G. Bayreuther, and D. Weiss, *J. Appl. Phys.* **91**(10), 7995 (2002).
- ⁵² P.-O. Jubert, J.-C. Toussaint, O. Fruchart, C. Meyer, and Y. Samson, *Europhys. Lett.* **63**, 132 (2003).
- ⁵³ R. Hertel, O. Fruchart, S. Cherifi, P.-O. Jubert, S. Heun, A. Locatelli, and J. Kirschner, *Phys. Rev. B* **72**, 214409 (2005).
- ⁵⁴ T. Shinjo, T. Okuno, R. Hassdorf, K. Shigeto, and T. Ono, *Science* **289**, 930 (2000).
- ⁵⁵ J. P. Park, P. Eames, D. M. Engebretson, J. Berezovsky, and P. A. Crowell, *Phys. Rev. B* **67**, 020403 (2003).
- ⁵⁶ T. Nagai, H. Yamada, M. Konoto, T. Arima, M. Kawasaki, K. Kimoto, Y. Matsui, and Y. Tokura, *Phys. Rev. B* **78**, 180414 (2008).
- ⁵⁷ N. D. Mermin, *Rev. Mod. Phys.* **51**, 591 (1979).
- ⁵⁸ J. M. Gregg, *Ferroelectrics* **433**, 74 (2012).
- ⁵⁹ S. Mühlbauer, B. Binz, F. Jonietz, C. Pfleiderer, A. Rosch, A. Neubauer, R. Georgii, and P. Böni, *Science* **323**(5916), 915 (2009).
- ⁶⁰ X. Z. Yu, Y. Onose, N. Kanazawa, J. H. Park, J. H. Han, Y. Matsui, N. Nagaosa, and Y. Tokura, *Nature* **465**, 901 (2010).
- ⁶¹ S. K. Streiffner, J. A. Eastman, D. D. Fong, C. Thompson, A. Munkholm, M. V. Ramana Murty, O. Auciello, G. R. Bai, and G. B. Stephenson, *Phys. Rev. Lett.* **89**, 067601 (2002).
- ⁶² D. D. Fong, G. B. Stephenson, S. K. Streiffner, J. A. Eastman, O. Auciello, P. H. Fuoss, and C. Thompson, *Science* **304**, 1650 (2004).
- ⁶³ H. Fu and L. Bellaiche, *Phys. Rev. Lett.* **91**, 257601 (2003).
- ⁶⁴ M. G. Stachiotti and M. Sepiarsky, *Phys. Rev. Lett.* **106**, 137601 (2011).
- ⁶⁵ J. Seidal *et al.*, *Adv. Electron. Mater.* **2**, 1500292 (2016).
- ⁶⁶ C.-L. Jia *et al.*, *Science* **331**, 1420 (2011).
- ⁶⁷ C. Nelson *et al.*, *Nano Lett.* **11**, 828 (2011).

- ⁶⁸ A. R. Damodaran *et al.*, [Nat. Mater.](#) **16**, 1003 (2017).
- ⁶⁹ S. Prosandeev *et al.*, [Phys. Rev. B](#) **87**, 195111 (2013).
- ⁷⁰ H. Smid, [J. Phys.: Condens. Matter](#) **20**, 434201 (2008).
- ⁷¹ P. Shafer *et al.*, [Proc. Nat. Acad. Sci. U. S. A.](#) **115**, 915 (2018).
- ⁷² M. Jaafar, R. Yanes, D. Perez de Lara, O. Chubykalo-Fesenko, A. Asenjo, E. M. Gonzalez, J. V. Anguita, M. Vasquez, and J. L. Vicent, [Phys. Rev. B](#) **81**, 054439 (2010).
- ⁷³ K. Yamada, S. Kasai, Y. Nakatani, K. Kobayashi, H. Kohnno, A. Thiaville, and T. Ono, [Nat. Mater.](#) **6**, 270 (2007).
- ⁷⁴ R. P. Beardsley, S. Bowe, D. E. Parkes, C. Reardon, K. W. Edmonds, B. L. Gallagher, S. A. Cavill, and A. W. Rushforth, [Sci. Rep.](#) **7**, 7613 (2017).
- ⁷⁵ R. Tomasello *et al.*, [Sci. Rep.](#) **4**, 6784 (2014).
- ⁷⁶ S. S. P. Parkin, M. Hayashi, and L. Thomas, [Science](#) **320**, 190 (2008).